ROSE/TN/97–2
Revised: December 1999

The NIEL scaling hypothesis applied to neutron spectra of irradiation facilities and in the ATLAS and CMS SCT[1]

Angela Vasilescu

INPE Bucharest, Romania, E-mail: angela@ifin.nipne.ro

In the radiation hardness studies of silicon detectors macroscopic and microscopic quantities are analysed with respect to radiation fluence. The irradiation facilities used for such investigations are very different as to spectral distribution and particle type, and it is natural to seek for a suitable normalisation by which these differences are cancelled out and reliable comparisons between results with different sources can be achieved.

The irradiation test results meant to be the basis for the design and simulation of detector behaviour at very high energies are carried out in beams with various spectra, starting with monoenergetic beams to wide spectrum spallation sources, e.g. for neutrons. They differ also from the actual radiation fields expected in the final experimental environments in which the detectors are supposed eventually to work. The transfer of the test results to the experiment and the intercorrelation and unification of the test data coming from different irradiation facilities are essential scopes of the radiation damage studies.

The correlation of the experimental data is done in the frame-work of the NIEL (Non Ionising Energy Loss) scaling hypothesis.

1 The energy scaling of damage effects

The NIEL scaling can be reduced to the definition of the 1 MeV equivalent neutron fluence which produces the same damage as an arbitrary beam with a certain spectral distribution $\phi(E)$ and of fluence Φ:

$$\Phi_{eq}^{1MeV} = \kappa\Phi \tag{1}$$

κ is called the hardness parameter and is defined as:

$$\kappa = \frac{EDK}{EDK(1\ MeV)} \tag{2}$$

with EDK the energy spectrum averaged displacement KERMA:

$$EDK = \frac{\int D(E)\phi(E)dE}{\int \phi(E)dE} \tag{3}$$

where $\phi(E)$ is the differential flux and

$$D(E) = \sum_k \sigma_k(E) \int dE_R f_k(E, E_R) P(E_R) \tag{4}$$

the displacement KERMA or the damage function for the energy E of the incident particle, σ_k the cross section for reaction k, $f_k(E, E_R)$ the probability of the incident particle to produce a recoil of energy E_R in reaction k, and $P(E_R)$ the partition function (the part of the recoil energy deposited in displacements). EDK(1 MeV)=95 MeV mb [3]. The integration is done over the whole energy range.

[1] This report summarizes a part of the PhD Thesis [1] presented in 1997 at IAP Bucharest (in Romanian). For general reference, a summary is available in English. A second part of the thesis, closely related to this report is an overview on the radiation environment at ATLAS and CMS and on irradiation sources, available as [2]. This latter report gives a complete reference to the different irradiation facilities.

The detailed analysis of the different quantities in the definition of the hardness parameter κ was motivated by the discrepancies found in the experimental data, in an attempt of intercomparison (fig. 1 and [4, 5]), based on the published values of κ [6, 7, 8, 9, 10, 11].

In the following discussion of the scaling hypothesis, the special case of neutrons will be considered. The definitions above hold for other particles, too.

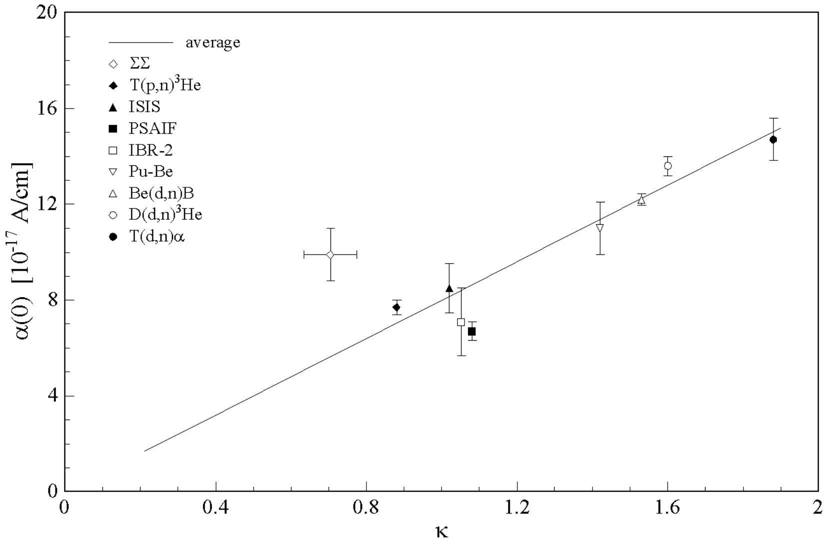

Figure 1: Systematic on $\alpha(0)$ damage constant values from literature and its dependence on the hardness parameter κ (1994). The continuous line is an average estimated by [7].

1.1 Partition function

Neutron induced damage in solids appears from direct collisions producing displacements and nuclear reactions resulting in high energy recoils. These cause ionisation and excitations of the atoms in the irradiated material, as well as elastic and inelastic scattering producing further dislocations of the atoms from their sites in the lattice. The effects of the interaction of the primary particle with the lattice are mainly residual ionisation and the creation of disordered regions and complex defects, due to atomic displacements directly or after migration and final recombination of Frenkel defects with other impurities. Ionisation is a transient effect in silicon, it does not contribute to permanent damage. Displacements appear in cascades and can generate permanent defects. Their dynamics is described in MC simulation [12, 13] and transport calculations.

The partition of the primary recoil energy E_R between electronic excitation and atomic displacements is reflected in the definition of the damage function $D(E)$ (equation 4) via $P(E_R)$, the partition function. The ratio $P(E_R)/E_R$ is called damage efficiency. The partition function, calculated in the LSS (Lindhard screened potential scattering) theory [14], based on the Thomas–Fermi model, and further developments [15], is given by:

$$P(E_R) = \frac{E_R}{1 + F_L(3.4008\epsilon^{1/6} + 0.40244\epsilon^{3/4} + \epsilon)} \tag{5}$$

for $E_R \geq E_d$, the minimum energy of the recoil required to produce a displacement, and $P(E_R)$=0 elsewhere; with

$$\epsilon = \frac{E_R}{E_L} \tag{6}$$

and

$$E_L = 30.724 Z_R Z_L (Z_R^{2/3} + Z_L^{2/3})^{1/2} (A_R + A_L)/A_L$$

$$F_L = \frac{0.0793 Z_R^{2/3} Z_L^{1/2}(A_R + A_L)^{3/2}}{(Z_R^{2/3} + Z_L^{2/3})^{3/4} A_R^{3/2} A_L^{1/2}}$$

Here L stands for lattice, and R for recoil.

For silicon E_d is taken conventionally 25 eV (a value as good as that could be 15 or 20 eV as well). For Si recoils in silicon Z_R=Z_L=14, A_R=A_L=28, and we get the partition function $P(E_R)$ plotted in figure 2.

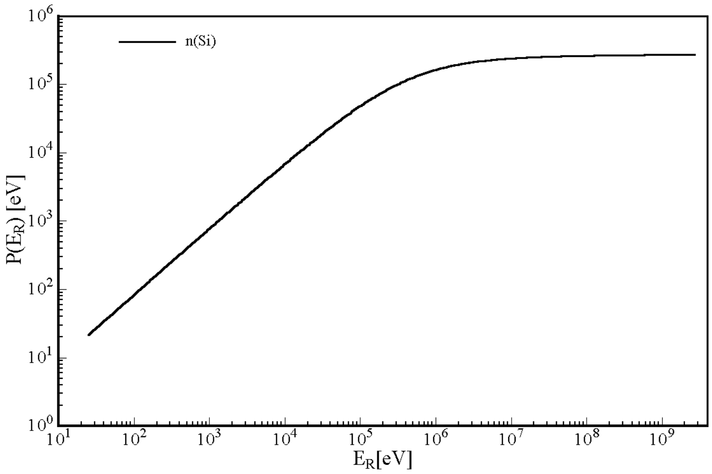

Figure 2: Damage efficiency in silicon

1.2 Damage function

The evaluation of the damage function in silicon has been a subject of interest with military application, that is why the data published in literature were rather poor and incomplete. The first attempts to correlate the radiation effects and implicitly to describe them with a damage function go back to a series of experimental papers in the 80's [16]–[21]. All these papers and especially reference [21] have inspired the calculations of the displacement function to energies above 20 MeV published by van Ginneken [22]. A table of values for the damage function and the recipe for the scaling calculations to 1 MeV equivalent fluence have been standardized (ASTM E722–85 [3]). Later, new tables have been calculated by Lazo et al [23] and Ougouag et al [24], for the damage function for neutrons up to 18 MeV, based on the so-called 600-group structure. These values have been adopted in the revision of 1993 of the ASTM E722, too.

In references [23, 24] the interaction cross sections have been taken into account via the NJOY computer code [25], based on the ENDF/B–V nuclear data compilation, distributed by Brookhaven National Laboratory [26]. All reaction cross sections are included, starting with elastic and inelastic scattering, as well as (n,γ), (n,α), (n,2n) and other reactions. Figure 3 presents the Ougouag and van Ginneken damage functions versus incident energy.

As it can be seen from the figure, the units for the two damage functions are different. Following the definition from [22]:

$$\frac{dE}{dx}|_{n.i.} = N \sum_{Z,A} \int_{E_R^{min}}^{E_R^{max}} \frac{d\sigma}{dE_R} P(E_R) dE_R \tag{7}$$

with

$$N = \frac{N_A}{A}\rho$$

we can identify the sum over Z and A with the sum over all reactions k in Eq. 4, so that:

$$NIEL = \frac{dE}{d(\rho x)}|_{n.i.} = \frac{N_A}{A} D(E) \tag{8}$$

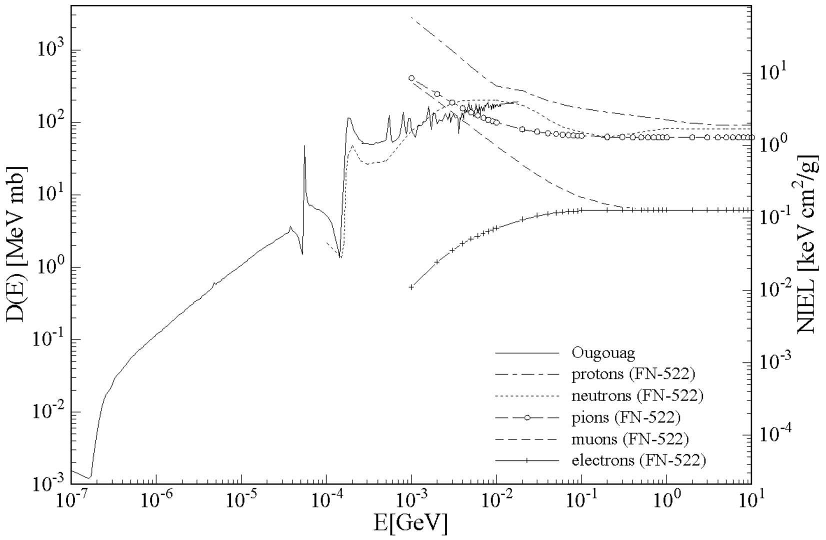

Figure 3: Damage functions in silicon: $D(E)$-Ougouag and NIEL-FN-522. $D(E)$ is in MeV mb (left y axis), NIEL$_G$ (van Ginneken) is given for protons, pions, muons, neutrons and electrons in keV cm^2/g (right y axis)

For silicon A=28.086 g/mol and consequently

$$100 \text{ MeV mb}=2.144 \text{ keV cm}^2/\text{g}$$

The above unit transformation is used to couple the two damage functions for neutrons above 18 MeV.

It is important to mention that Ougouag's $D(E)$ function [24] was calculated starting with 10^{-4} eV, the lower limit in the cross section data compilation [26]. The damage functions from [23] and [24] differ only within less than 1%, the second set of data being more detailed. This is the reason why all the calculations in the present work have been performed with the Ougouag $D(E)$ function up to 18 MeV, and van Ginneken's function above 20 MeV.

In fig. 4 Ougouag's damage function is given for the entire energy range.

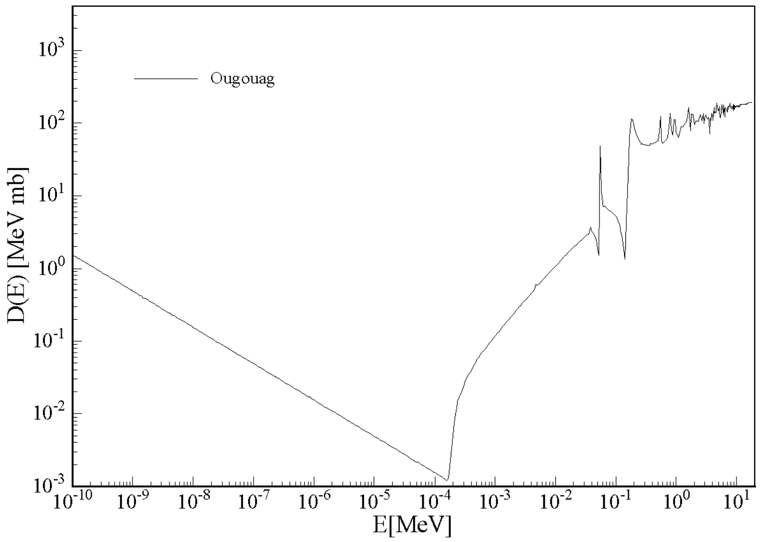

Figure 4: The $D(E)$ damage function – after Ougouag et al. [24]

Van Ginneken's results [22] are based on the experimental data and the estimates from [21], extended by calculations to the whole energy range, using supplementary hypotheses. More exact or reliable calculations or experimental proofs of the behaviour of the damage function above 18 MeV do not exist. Van Ginneken's primary assumptions are rather simplifying. Experimental data on neutron cross sections in the high energy region are missing, and van Ginneken calculates the NIEL_G damage function by "matching" the neutron values to the proton cross section data minus the Coulomb interaction, a quite rough approximation. The NIEL_G curve decreases from 15 to 100 MeV, then increases again to a plateau approximately equal to the proton NIEL at 10 GeV. In the Ougouag function the tendency is a clear increase above 15 MeV, therefore a natural question is if the van Ginneken estimation could be checked experimentally.

For the validation of the NIEL damage function in the energy region around 20 MeV a test experiment to be carried out in the near future has been proposed. This energy range is especially interesting as the most recent ASTM data present a slow increase of the NIEL function with energy, while the van Ginneken curve drops down after 15 MeV. An adequate neutron generator to be used in this test should produce a monoenergetic neutron beam, uncontaminated with other particles or energies. Such a possibility is the $T(d,n)^4He$ reaction. The first excited level in ^4He is situated at 20.1 MeV (0^+), followed by levels at 21.1 (0^-) and 22.1 (2^-). The energy of reaction for $T(d,n)^4He$ is Q=17.6 MeV. A simple kinematical calculation shows that with an incident deuteron beam of 4.15 MeV, in principle easy to obtain from a small cyclotron or low energy van de Graaff, neutrons of 21 MeV would result. Using the reaction mentioned above, we could, in principle, test the NIEL damage function of van Ginneken in the critical energy region of 15–20 MeV, where the van Ginneken and ASTM data differ not only in absolute value, but also in the energy dependence.

The contribution to κ for the different spectra extending above 20 MeV and its dependence on the shape of the NIEL_G curve were estimated in a comparison with a constant damage function above 18 MeV, and a linearly increasing damage function towards the 10 GeV value. The results obtained are given in subsection 2.4.

1.3 Integration limits. Second order effects

In the estimation of the κ hardness parameter for the sources used in radiation damage tests, different authors have used the various damage functions presented above. In some papers the damage function from ASTM E 722-85 has been used, which is not correct, as has been proved experimentally in [7]. A more complicated problem is related to the choice of the integration limits in the spectrum integrals of equation 3. For instance the same ASTM version (1985) proposes the low integration limit E_{min} = 10 keV, for "historical reasons", but without any physical motivation for our application. It comes from the fact that this standard has been initially written for electronic components to be tested in fast reactors, where the 10 keV limit was a good approximation. Another possible choice for E_{min} is the elastic threshold energy 190 eV, corresponding to the minimum neutron energy to produce a recoil of E_d=25 eV by elastic scattering. This choice is also arbitrary, as lower energy neutrons can also produce displacements, as it will be shown further. At PSAIF a pragmatic value of 140 keV has been used for the low cut of the total fluence integral [27].

If we plot the neutron spectra folded with the damage function $D(E)$ (fig. 5) and compare to the respective spectra, we see that the areas under the respective curves are different, depending on the E_{min} cut. This will determine variations in the values of κ with the different extension of the spectrum on the energy scale.

The high number of low energy neutrons do not add a large contribution to the total damage, but the fluence coming from these neutrons (the denominator in (3)) contributes substantially to the changes in the κ value: e.g. the fluence calculated integrating the ISIS spectrum for the position at 8 cm represents 50.5% of the total spectrum, at 68 cm 15% of the integral fluence, and at PSAIF only 3.3% of the total number of neutrons are in the energy range above 100 keV.

From the original papers on damage functions [23, 24], and figure 4, respectively, we can see that the kinematical limit imposed (190 eV) by the elastic threshold calculated according to the energy necessary to produce a displacement (25 eV) corresponds to the minimum in the damage curve. However the damage functions continue below this limit with the so-called "disappearance part"[23],

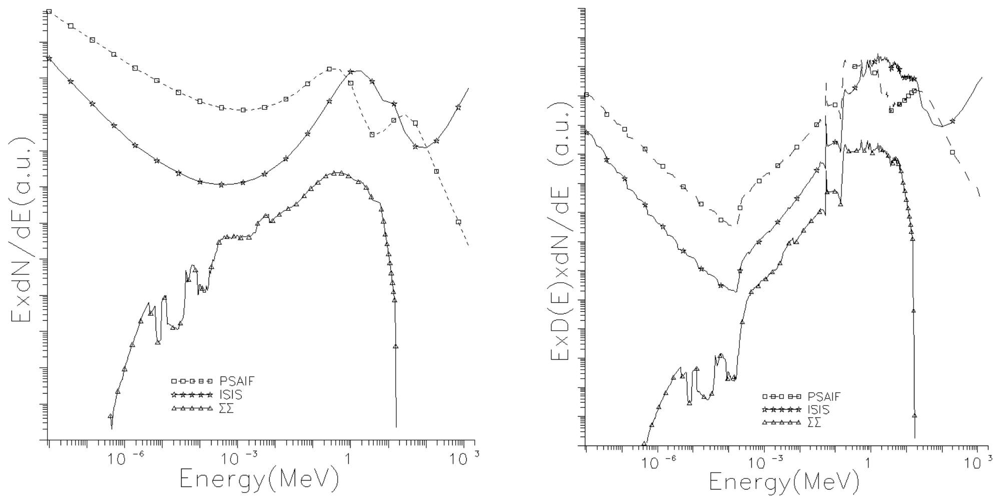

Figure 5: Neutron spectra (left side) and folded spectra (right side). The lethargy plot representation given here has the advantage to compress the x axis. If the y axis were linear, the area under the curves would be equal to the integral corresponding to the considered energy limits.

down to the limit of cross section data in ENDF–B/V [26]. This part of the cross section curves has been by mistake considered to be unable to produce atomic displacements, confusion due partly to the unfortunate term of "disappearance" part of the function. From the analysis of the cross section data in silicon, one can see that in the low energy range the only positive Q-value nuclear reaction is (n,γ) with Q=8.475 MeV. A simple kinematical estimate gives for the recoil energy of Si 1.28 keV, well above the 25 eV limit. If we multiply now the (n,γ) cross section by the 1 keV energy available for displacements, according to the Lindhard theory, we reproduce the damage function $D(E)$ in this energy region. This interpretation was verified in direct discussions with the authors of the damage function calculations [28]. At the same time the origin of the term "disappearance" was clarified – it is related to the fact that the neutron is absorbed (disappears from the final products) in the reaction.

The NJOY computer code does not take into account the fact that in the (n,γ) reaction a two component gamma cascade (3 and 5 MeV) is produced, but treats the recoil as due to a single 8.475 MeV gamma ray.

It should be also noted that the recombination of the initial Frenkel defects has been neglected in the theory so far. It is to be expected that the recombination probability is energy dependent, higher for low energy transfers, and for low energy recoils this effect would reduce the damage function accordingly.

The treatment of the displacement cross section based on the NJOY calculations and the ENDF–B/V data considers all the reactions existing in the compilation. For the calculations a global model based on the Lindhard (LSS) theory is assumed [14, 12], restricted only to direct recoils.

Looking carefully at the list of nuclear reaction channels, opening with increasing neutron energy, we notice some reactions worth to be mentioned:

1. Si(n,γ) This reaction has been already discussed above. Roughly $E_\gamma = 8.5$ MeV, and the energy transferred to the Si–recoil is about 1 keV (40 displacements!). As will be seen later, the overall effect on the total produced damage is low.

2. ^{28}Si(n,p)^{28}Al begins to be important above E_n ~4 MeV (Q=–3.85 MeV). The displacements due to the ^{28}Al and the proton recoils have been considered in the displacement function, but we should note that ^{28}Al is a beta emitter with a halflife of 2.3 h (^{28}Al$\rightarrow \beta +^{28}$Si) with $E_\beta^{max}=$ 4.65 MeV. The emitted electron produces further recoils of ^{28}Si in the keV range, a contribution to the damage to be evaluated.

3. ^{28}Si(n,d)^{27}Al with Q=–9.36 MeV is to be considered above 10 MeV. The resulting nucleus is an acceptor, but, due to the low cross section (of about 10 mb), the concentration produced in an irradiation of 10^{14} n/cm^2 fluence is only of the order of $5 \cdot 10^{10}$cm^{-3} which is not significant.

4. ^{28}Si(n,α)^{25}Mg (Q=–2.65 MeV) begins to be important above 3 MeV. ^{25}Mg is a donor[29], the cross-section for its production is about 200 mb at 8 MeV and the concentration produced by a 10^{14} n/cm^2 fluence is already significant (10^{12}cm^{-3}). This reaction has been used for fast neutron transmutation.

Above 20 MeV more and more reaction channels are open, e.g. (n,2n) already at 17.2 MeV: their analysis could be important for sources with a dominant high energy part in the spectrum.

2 The hardness parameter κ

2.1 κ in literature. Discrepancies

At an attentive reading of the published material on radiation hardness of silicon detectors for future experiments at LHC, one can see that the estimates for the hardness parameter at certain sources differ in time. This is the case for ISIS and PSAIF, especially. Thus, for the ISIS spallation source at Rutherford Appleton Laboratories, the first published κ value is 1.5±0.2 [9, 10]. Later estimates situate κ between 1.07 and 1.5, depending on distance to the source and the integration limits used [11]. The RD2 collaboration gives the corrected value of 1.02 [8].

About the PSAIF at CERN several papers claim that it has an energy equivalent to 1 MeV ($\kappa \sim$1). An estimate in [6] gives κ=1.08. With the initial values for κ in the systematics in fig. 1, the $\alpha(0)$ values measured in tests at these sources deviate considerably from the average.

Previous estimates [5] gave $\kappa(ISIS)_{av}$=1.10±0.06 and $\kappa(PSAIF)$=0.49±0.02, calculated from the elastic threshold, and $\kappa(PSAIF)_{>140keV}$=0.74±0.04, with the arbitrary cut used in the fluence integration. These results differ from the previously published ones by other authors, mainly for PSAIF. Coming back to the systematics on the $\alpha(0)$ damage constant, the latter κ values improve the situation, meaning that the scaling hypothesis is correct and it is useful in the correlation of the experimental results and their extrapolation to the simulated spectra in the HEP detectors at high luminosity.

The discrepancies in the estimated values presented above are due to the different energy cuts used, but possibly also to some mistakes in the earlier interpretation of the spectra or of the recipe for the calculation of κ. The ISIS and PSAIF spectra have been calculated with the same unfolding code LOUHI, on results from activation foil measurements.

In the following the calculations of the hardness parameter performed in this work will be presented in detail, together with the results obtained for each of the neutron sources used.

2.2 Folding methods

The different representations of the spectra of the sources studied created some problems in the evaluation of the hardness parameter. Some spectra are presented as tables in bins, others as continuous functions, depending on the methods of measurement and calculation used. Details on these methods are not explicitly given in the papers (usually internal reports) which describe the irradiation facilities.

The damage functions are continuous functions, tabulated in unequal steps on different energy ranges.

It is clear that at the calculation of the hardness parameter some averaging and interpolations have to be done in the folding procedure, as well as in the calculation of the integrals on the spectrum. In order to avoid the introduction of unphysical effects, resulting from mathematical artefacts, the folding method has been separated on two main cases: "continuous" spectra and binned spectra.

The initial computer codes used linear interpolation in between the points, on the displacement cross section data $D(E)$, as well as on the spectral distribution. The integration method was the simple trapezoidal integration. Linear interpolation underestimated the decreasing parts of the spectra and overestimated the increasing ones, especially in the parts with few experimental points. Comparative

Source	E_{min}[MeV]	E_{max}[MeV]	κ	flux [a.u.]	<E>[MeV]
IBR	0.5	17	1.05	3.94×10^{11}	1.65
Lowell	0.03	1.825	0.895	2.49×10^{11}	1.06
ΣΣ	4.25×10^{-7}	17.9	0.663	7.61×10^{5}	0.82
	1.9×10^{-4}	17.9	0.663	7.61×10^{5}	0.82
PSAIF	10^{-8}	100	0.025	1.23×10^{10}	0.062
	1.9×10^{-4}	100	0.502	5.81×10^{8}	1.32
	0.140	100	0.747	3.81×10^{8}	1.99
PSAIF	10^{-8}	1400	0.025	1.23×10^{10}	0.072
	1.9×10^{-4}	1400	0.503	5.82×10^{8}	1.52
	0.140	1400	0.747	3.82×10^{8}	2.29
ISIS 8 cm	10^{-8}	100	0.546	7.71×10^{8}	1.49
	1.9×10^{-4}	100	1.102	3.81×10^{8}	3.02
ISIS 8 cm	10^{-8}	1400	0.555	8.01×10^{8}	36.1
	1.9×10^{-4}	1400	1.080	4.11×10^{8}	70.3
ISIS 38 cm	10^{-8}	100	0.231	4.45×10^{8}	0.79
	1.9×10^{-4}	100	1.051	9.74×10^{7}	3.62
ISIS 38 cm	10^{-8}	1400	0.232	4.46×10^{7}	2.06
	1.9×10^{-4}	1400	1.046	9.88×10^{7}	9.29

Table 1: Main parameters of sources calculated with the linear interpolation method. For PSAIF and ISIS results are given for the whole spectrum and with a high energy cut at E_{max}=100 MeV.

Source	E_{min}[MeV]	E_{max}[MeV]	κ	flux[a.u.]	<E>[MeV]
IBR	0.5	17	1.05	3.94×10^{11}	1.60
Lowell	0.03	1.825	0.895	2.49×10^{11}	1.06
ΣΣ	4.25×10^{-7}	17.9	0.663	7.61×10^{5}	0.82
	1.9×10^{-4}	17.9	0.663	7.61×10^{5}	0.82
PSAIF	10^{-8}	100	0.025	1.23×10^{10}	0.057
	1.9×10^{-4}	100	0.517	5.81×10^{8}	1.21
	0.140	100	0.769	3.81×10^{8}	1.81
PSAIF	10^{-8}	1400	0.025	1.23×10^{10}	0.066
	1.9×10^{-4}	1400	0.517	5.82×10^{8}	1.40
	0.140	1400	0.769	3.82×10^{8}	2.11
ISIS 8 cm	10^{-8}	100	0.550	7.71×10^{8}	1.32
	1.9×10^{-4}	100	1.110	3.81×10^{8}	2.67
ISIS 8 cm	10^{-8}	1400	0.559	8.01×10^{8}	37.2
	1.9×10^{-4}	1400	1.087	4.11×10^{8}	72.5
ISIS 38 cm	10^{-8}	100	0.234	4.45×10^{8}	0.71
	1.9×10^{-4}	100	1.063	9.74×10^{7}	3.25
ISIS 38 cm	10^{-8}	1400	0.235	4.46×10^{8}	1.94
	1.9×10^{-4}	1400	1.058	9.88×10^{7}	8.75

Table 2: Results calculated by linear interpolation with smoothing on energy intervals corresponding to the steps in the damage function $D(E)$. For PSAIF and ISIS the results are given for the whole spectra and with a high energy cut at E_{max}=100 MeV.

studies of linear and logarithmic interpolation for ISIS and PSAIF have been performed, as these spectra are given in logarithmic steps. The log–interpolation underestimated the increasing part and overestimated the decreasing part of the distributions. Detailed scan on restricted energy ranges followed by graphic comparisons has been done in order to establish the interpolation and smoothing methods with the best accuracy. For the spectra presented in small step tables, spaced linearly on the energy scale, the agreement of the results is very good, independent of the method, which means that the simplest linear interpolation method is good enough for these calculations. The errors introduced by the computational method are small compared to the imprecision in the determination of the spectral distribution. The linear interpolation method works well for the spectra at $\Sigma\Sigma$, IBR–2, Lowell (see tables 1 and 2).

The case of the ISIS and PSAIF spallation sources is more complicated. In order to diminish the estimation errors at these spectra, the solution found was to calculate the distribution function with spline interpolation on the spectra, followed by the folding with the displacement function, with local linear interpolation where necessary. Practically the distribution is a fine step continuous function and the folded function follows the fluctuations in the damage function.

For the binned spectra, averaging of the damage function on the bins had to be performed, and the integral is calculated by summing up the contributions of all the bins, with smoothing the damage functions on the corresponding energy regions. This method has been applied for the Be(d,n) source at PTB Braunschweig (table 3) and at the estimation of the hardness parameter for the simulated spectra in ATLAS and CMS (section 3).

2.3 κ for currently used test facilities

This subsection gives the tables of values for the hardness parameter κ for the neutron sources currently used in radiation damage studies of silicon detectors, obtained with the computational methods described above. The results are grouped as below:

- with linear interpolation method: table 1
- with smoothing : table 2
- results on the Be(d,n) source are given separately (table 3).

E_{min}[MeV]	E_{max}[MeV]	κ	fluence[cm^{-2}]	<E>[MeV]	method
0.7	18.5	1.48	2.57×10^{16}	5.44	(1)
0.7	18.5	1.48	2.57×10^{16}	5.44	(2)
0.6	18.45	1.47	2.60×10^{4}	5.39	(3a)
0.05	18.45	1.47	1.30×10^{4}	5.39	(3b)
0.05	18.45	1.45	1.23×10^{4}	5.21	(3c)

Table 3: Calculations of the hardness parameter for the Be(d,n) source at PTB: (1) linear interpolation on continuous function (old data), (2) interpolation and smoothing on energy intervals corresponding to the damage function steps, (3) binned spectra calculations; (a) and (b) represent two data sets with E_d=13.54 MeV, and (c) a data set with E_d=13.26 MeV.

The maximum error estimated for κ is less than 5%.

The ISIS and PSAIF sources will be discussed in further detail in the next subsection.

2.4 Errors introduced by energy cuts. Relative damage

Tables 1 and 2 contain only a selection of the results obtained in the calculations performed. In the study of the variation of the hardness parameter, average energy and fluence, the respective values have been calculated for different energy cuts: the whole spectrum and low energy cuts at every decade up to 100 keV. In an initial analysis [5], for the PSAIF and ISIS the effect of an arbitrary high energy cut at E_{max}=100 MeV has been analysed (which is presented in the tables), considering that the number of neutrons above this limit is negligible. It results from the calculations that, indeed, those neutrons do not influence appreciably the damage. The same study estimated the relative contribution to damage of the part of the spectrum for which κ has been calculated, and the results are given in table 4. A further discussion on the high energy limit correlated with the physical background is given in this work.

	all spectrum	$E_{max}=$ 100 MeV*	$E_{min}=$ 1 eV	10 eV	190 eV	1 keV	10 keV	100 keV
κ								
ΣΣ	0.66	–	0.66	0.66	0.66	0.67	0.69	0.78
ISIS(8cm)	0.56	0.55	1.09	1.10	1.10	1.10	1.10	1.11
PSAIF	0.024	0.024	0.26	0.41	0.49	0.52	0.55	0.68
Φ[%]								
ΣΣ	100	–	100	100	100	99.3	96.6	84.4
ISIS(8cm)	100	94.8	50.8	50.4	50.4	50.3	50.3	49.8
PSAIF	100	100	9.0	5.7	4.7	4.5	4.2	3.3
Relative	damage[%]							
ΣΣ	100	–	100	100	100	100	100	98.9
ISIS(8cm)	100	100	99.4	99.4	99.5	99.5	99.8	99.5
PSAIF	100	100	96.2	96.3	96.1	96.2	96.2	94.3

Table 4: The variation of the hardness parameter κ with the integration limits. The percent fluence and relative damage corresponding to each energy cut. The column marked with (*) is missing for the ΣΣ source, as its spectrum ends at about 17 MeV.

The dependence of the hardness parameter on the limits of integration for wide neutron sources is given in a diagram in figure 6.

In subsection 2.2 the imprecision of the folding methods has been widely discussed for PSAIF and ISIS. Figure 7 shows in a suggestive comparison the differences in the area with linear and spline interpolation.

Among the neutron sources used for damage studies, PSAIF and ISIS are the only ones with spectra extending above 20 MeV, the energy range covered so far only by van Ginneken's NIEL damage function [22]. As already commented in subsection 1.2, van Ginneken's evaluation is based on simplifying hypotheses. As in the collider experiments spectra will extend to the GeV region, the discussion of this energy region is very important.

κ has been evaluated for ISIS and PSAIF, calculated with the spectra obtained in spline interpolation, in the following variants: with the damage function $D(E)$+NIEL (a) and with a $D(E)$+ modified NIEL function: (b)– a constant equal to the last value in the list of $D(E)$ by Ougouag [24] and (c)– decreasing to the limit value equal to the value at 10 GeV in the van Ginneken data. The results obtained are given in table 5.

spectrum	(a)	(b)	(c)
ISIS 8 cm	0.578	0.636	0.632
38 cm	0.256	0.265	0.265
68 cm	0.143	0.150	0.149
PSAIF	0.0255	0.0263	0.0263

Table 5: κ values on the whole spectrum with different variants of the damage function above 20 MeV

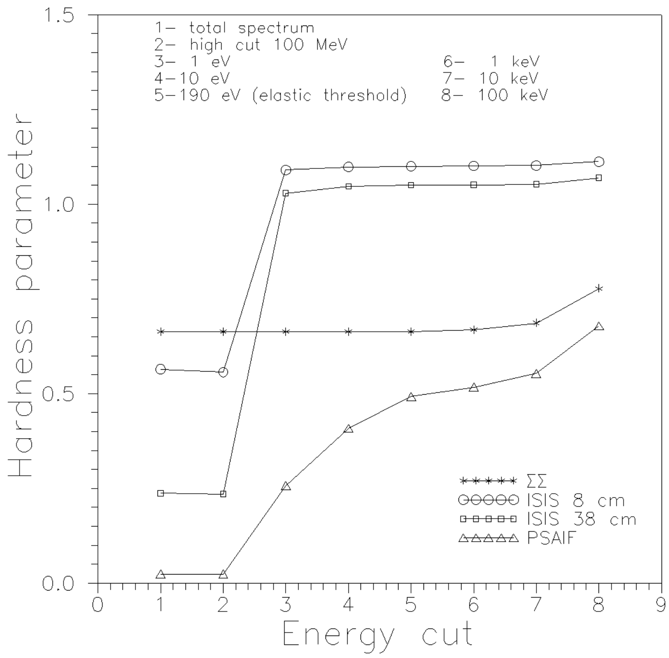

Figure 6: The dependence of κ on the limits of integration for wide spectrum neutron sources

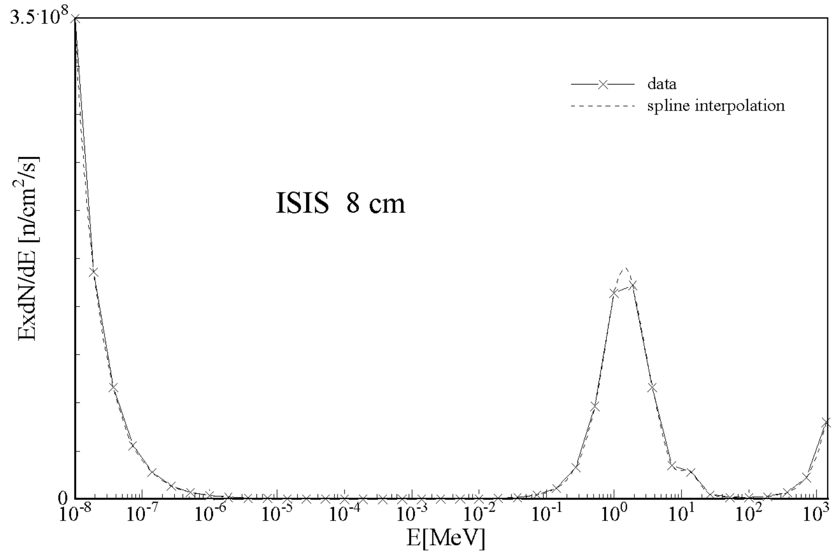

Figure 7: ISIS neutron spectrum at 8 cm from the collector. Comparison with spline interpolation.

As expected, the modified NIEL functions give higher contributions to κ, and the relative weight of this contribution depends on the spectral distribution. Because in the LHC environment the high energy part of the spectra is important, this energy region should be experimentally tested for the damage function.

A last comment is necessary related to ISIS. This refers to the high energy tail of the spectra for which, especially in the irradiation position at 8 cm, the unfolding program gives an increase in the number of neutrons at high energies which has no physical explanation.

At the ISIS facility there are two clear kinematical limits: one related to the energy of the injection into the synchrotron, at about 70 MeV, around which value most of the neutrons are produced, and the extraction energy (~800 MeV), above which limit the existence of neutrons is kinematically forbidden. As the spectra present fluences up to 1400 MeV and clearly such neutrons cannot be available, the spectrum has to be cut at the kinematical limit. The number and the contribution of these neutrons is small, as it has been seen in the preliminary study with the high energy cut at 100 MeV, but the knowledge of the correct value is necessary. This is why the new sets of values given in table 6 have been calculated for the ISIS spectra with high cuts at E_{max} = 76 and 720 MeV.

If at ISIS the kinematical limits are clear, allowing the interpretation of the spectra obtained with the LOUHI unfolding code from the activation data, in the case of PSAIF it would be necessary to remeasure the spectrum. The shape of the spectral distribution, with the two maxima has risen lots of discussions, as the second maximum might not have a physical explanation and could come from the artificial superposition of different energy regions, due to a defective renormalization.

If for the other sources used in radiation hardness studies the problem of the errors introduced by a defective scaling is minor, the recipe to consider at the wide spectrum sources is not as simple to decide. At the $\Sigma\Sigma$, the value of κ is constant over a wide range, so any energy cut is the same good up to 1 keV. The approximation induced in the spectrum and the difference in the relative damage are negligible.

At the ISIS spectra, if we consider the same integration limits for the two integrals in the formula for κ, and the corresponding physical high energy cut, the errors are very small. The only problem is the PSAIF.

However, it is possible to give a generalised recipe for the scaling, in which one can take into account the integration limits used at the fluence calculation. (This value is given by the people who run the irradiation facilities, using routine procedures.)

The new scaling recipe is based on the idea of replacing the real hardness parameter (calculated with folding over the whole spectrum) by an equivalent damage parameter $\kappa^{\dagger}$ estimated according to the artificial cut used in the fluence calculations.

This damage parameter is defined by:

$$\kappa^{\dagger}\Phi(> E_{min}) = [\kappa\Phi]^{tot} \tag{9}$$

The equivalent damage parameter differs from the hardness parameter κ calculated on the spectrum with the same energy cut E_{min}.

$$\kappa^{\dagger}(> E_{min}) = \kappa^{tot}\frac{\Phi^{tot}}{\Phi(> E_{min})} \tag{10}$$

The values for $\kappa^{\dagger}$ are given, together with the hardness parameter estimates κ for PSAIF and ISIS, in table 6. From this table we can see that the average values on the ISIS spectra for the two hardness parameters are

$$\kappa_{av}{=}1.00 \qquad (\kappa^{\dagger}_{av}{=}1.01)$$

These values are recommended to be used, as at the ISIS irradiation usually the information on the position of irradiation is missing. The difference between κ and $\kappa^{\dagger}$ of 1% is below the imprecision of the estimate (maximum 5%).

For PSAIF the value to be considered for the integral flux calculated from 140 keV is $\kappa^{\dagger}$=0.78.

E[MeV]	N_{TOT}	κ	$\kappa^\dagger$	N_{TOT}	κ	$\kappa^\dagger$
ISIS						
E_{max}:	720 MeV				76 MeV	
8 cm						
10^{-8}	6.80×10^{8}	0.57	–	6.70×10^{8}	0.57	–
10^{-7}	3.92×10^{8}	0.99	0.99	3.83×10^{8}	0.99	0.99
10^{-6}	3.68×10^{8}	1.05	1.05	3.58×10^{8}	1.06	1.06
10^{-5}	3.65×10^{8}	1.06	1.06	3.56×10^{8}	1.07	1.07
10^{-4}	3.65×10^{8}	1.06	1.06	3.55×10^{8}	1.07	1.07
1.9×10^{-4}	3.65×10^{8}	1.06	1.06	3.55×10^{8}	1.07	1.07
10^{-3}	3.64×10^{8}	1.06	1.06	3.55×10^{8}	1.07	1.07
10^{-2}	3.64×10^{8}	1.06	1.06	3.54×10^{8}	1.07	1.07
10^{-1}	3.60×10^{8}	1.07	1.08	3.51×10^{8}	1.08	1.08
38 cm						
10^{-8}	3.68×10^{8}	0.26	–	3.67×10^{8}	0.25	–
10^{-7}	1.11×10^{8}	0.85	0.85	1.10×10^{8}	0.85	0.85
10^{-6}	9.38×10^{7}	1.00	1.00	9.25×10^{7}	1.00	1.01
10^{-5}	9.23×10^{7}	1.02	1.02	9.10×10^{7}	1.02	1.03
10^{-4}	9.20×10^{7}	1.02	1.02	9.08×10^{7}	1.02	1.03
1.9×10^{-4}	9.20×10^{7}	1.02	1.02	9.08×10^{7}	1.02	1.03
10^{-3}	9.19×10^{7}	1.02	1.02	9.07×10^{7}	1.02	1.03
10^{-2}	9.18×10^{7}	1.02	1.03	9.05×10^{7}	1.03	1.03
10^{-1}	9.04×10^{7}	1.04	1.04	8.92×10^{7}	1.04	1.05
68 cm						
10^{-8}	3.29×10^{8}	0.14	–	3.28×10^{8}	0.14	–
10^{-7}	6.79×10^{7}	0.68	0.69	6.71×10^{7}	0.68	0.68
10^{-6}	5.15×10^{7}	0.90	0.91	5.07×10^{7}	0.90	0.91
10^{-5}	5.02×10^{7}	0.92	0.93	4.94×10^{7}	0.93	0.93
10^{-4}	5.00×10^{7}	0.93	0.93	4.92×10^{7}	0.93	0.93
1.9×10^{-4}	5.00×10^{7}	0.93	0.93	4.92×10^{7}	0.93	0.93
10^{-3}	5.00×10^{7}	0.93	0.93	4.92×10^{7}	0.93	0.93
10^{-2}	4.98×10^{7}	0.93	0.94	4.90×10^{7}	0.93	0.94
10^{-1}	4.88×10^{7}	0.95	0.96	4.80×10^{7}	0.95	0.96
PSAIF	total					
10^{-8}	1.06×10^{10}	0.026	–			
10^{-7}	2.67×10^{9}	0.098	0.10			
10^{-6}	1.00×10^{9}	0.26	0.27			
10^{-5}	6.51×10^{8}	0.40	0.42			
10^{-4}	5.55×10^{8}	0.47	0.49			
1.9×10^{-4}	5.42×10^{8}	0.48	0.50			
10^{-3}	5.17×10^{8}	0.51	0.52			
10^{-2}	4.83×10^{8}	0.54	0.56			
10^{-1}	3.85×10^{8}	0.67	0.70			
0.140	3.19×10^{8}	0.74	0.78			

Table 6: κ and $\kappa^\dagger$ hardness parameter values for the ISIS and PSAIF spallation sources, calculated on spline interpolated spectra

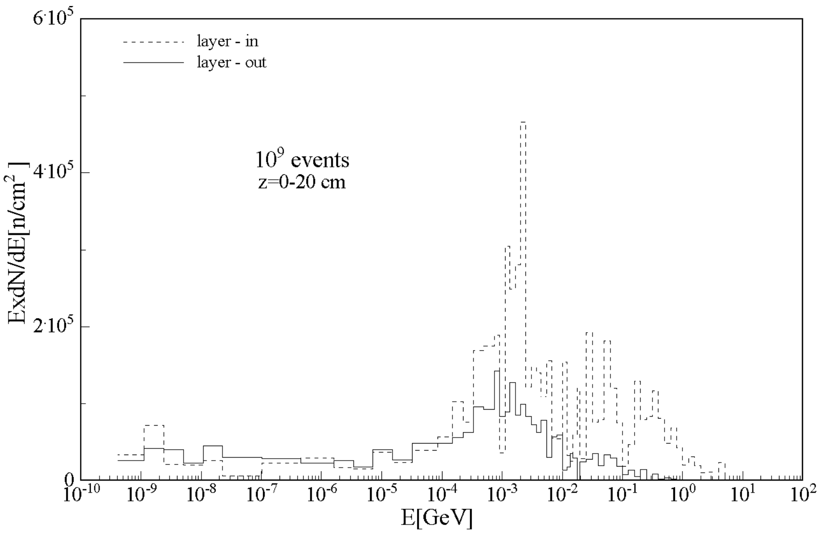

Figure 8: The CMS detector: Neutron spectrum in the outermost silicon microstrip layer, compared to the innermost one

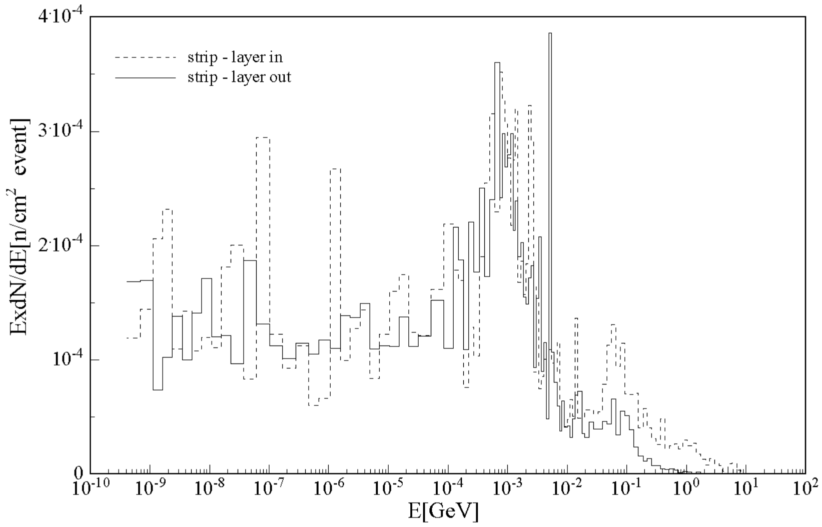

Figure 9: The ATLAS detector: Neutron spectrum for the outermost silicon microstrip layer in the Cosener's House layout. Comparison to the innermost layer. The data from A. Ferrari are integrated over z.

3 The hardness parameter for the CMS and ATLAS spectra

The spectra and the dose and fluence distributions in detector systems have been calculated by simulations based on the code FLUKA [31] by A. Ferrari [32, 33] and G. Gorfine [34] for ATLAS and M. Huhtinen [35, 37, 38] for CMS.

Except Ref. [34] the particles have been followed down to thermal energies (10^{-5} eV), but the statistics is relatively poor and the fluctuations large — the procedure of calculation is very time consuming. In [34] the low energy cut E_{min} was at 100 keV, to improve the statistics.

This energy cut is artificial and not supported by any physics background, at least for neutrons. This is clear from the shape of the damage function $D(E)$ in the energy region below 100 keV (see figures 3 and 4). As the albedo neutrons below this limit have a quite flat spectrum we can estimate the error introduced by the energy cut on the spectra given by A. Ferrari for ATLAS, by a similar calculation as the one on sources in subsection 2.4 and consider that the same is the error for the spectrum given in [34].

In [2] the particle spectra calculated for the CMS and ATLAS detectors have been presented, based on data from [34, 37]. Sometimes the details on the position to which the given spectra correspond is missing in the publications, or what is shown are averages. Complete simulations have been performed for different geometries and different points, at r and z distances chosen to be useful in the design of the detectors and the accepting of a certain layout. The data used in the present hardness parameter analysis come from the authors in 1995 and correspond to the results presented in the Technical Proposals of CMS and ATLAS [39, 40].

Figures 8 and 9 present the spectra corresponding to the CMS and ATLAS barrel silicon layers situated the farthest from the beam axis, together with the innermost silicon microstrip layers. (The upper energy end of the spectra should be compared for the different distances from the beam axis.)

In the energy range up to 100 MeV no essential differences in the neutron spectra can be noticed for a certain detector. Above 100 MeV, differences appear mostly for the extension of the spectra to high energies. They depend on the distance on r and z. The layers closer to the beam axis contain more energetic neutrons, for the layers situated farther the number of high energy neutrons is smaller. The effect is the same in both detectors: CMS and ATLAS. Figure 10 presents for illustration the high energy end of the neutron spectra for seven radial distances, corresponding approximately to the positions of the silicon layers in the Cosener's House layout in ATLAS.

In order to estimate the damage which will be produced in the silicon detectors, calculations of the hardness κ have been performed with different energy cuts, as in the case of the sources used for testing (section 2.3). The results obtained, including the percent damage corresponding to every energy cut, are presented in tables 7 and 8.

From these calculations we see that the approximation introduced by the energy cut at 100 keV in [34] is of about 2% (see table 8), which is certainly within the limit of errors in the calculations.

However a considerable uncertainty in the hardness factor and hence in the damage estimation is caused by fluctuations in the spectra due to the poor statistics of the MC calculations (figures 8, 9). An improvement would be very useful and lead to more reliable results.

The spectra contain a substantial part of neutrons with energies above 20 MeV, with a certain effect in the global damage. The error which appears from the lack of reliability of the damage function in this energy region is considered by some authors to be probably the most important of all [38, 41].

It is too early to consider the results of the simulations and damage calculations as final, as both detector designs are subject to changes. So, we consider that the results on 1 MeV equivalent fluence distributions can be used only as orientative, depending very much on the geometry and shielding.

Figure 11 gives an example of fluence values in CMS and ATLAS, on the data set used in the Technical Proposals (TP) [39, 40]. The latest SCT layout for ATLAS differs from the Cosener's House one (TP). But the changes to be expected in the spectra, hardness parameters and 1 MeV fluence values should not be very large as the quantities of material implied are small. Important changes appear in the spectra and fluences at the level of big components: calorimeters, pumps, etc.

For instance, for ATLAS a reduction by 10–17% of the yearly fluence in the TRT and the 4^{th} Si barrel layer is reported recently (June 1996), in a new constructive variant of the electromagnetic calorimeter [42].

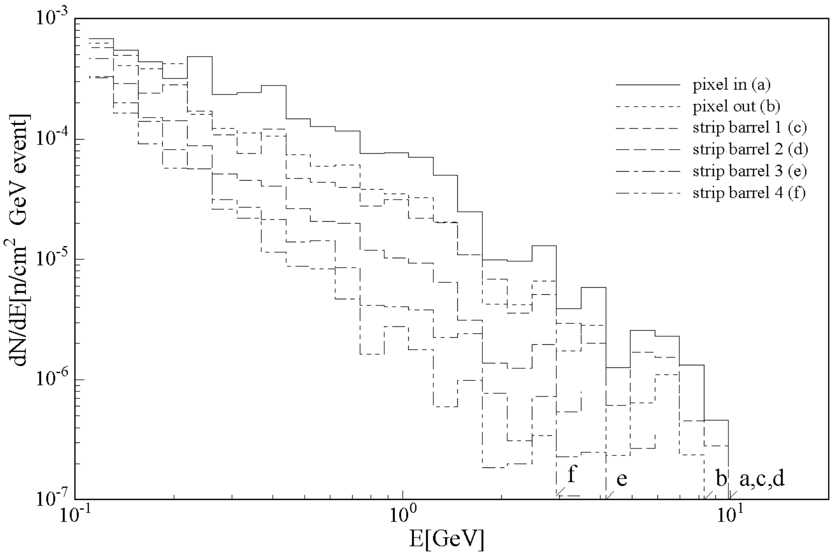

Figure 10: ATLAS: Neutron spectra in the pixel and barrel silicon layers in the Cosener's House layout at high energies.

r[cm]	z[cm]	E_{min}[MeV]	κ	fluence[10^6 cm^{-2}/10^9 events]	[%]	relative damage [%]
20	0–20	10^{-10}	0.398	2.89	100	100
	280–300		0.382	5.40	100	100
50	0–20		0.222	2.47	100	100
	280–300		0.286	4.07	100	100
100	0–20		0.193	2.25	100	100
	280–300		0.206	2.87	100	100
20	0–20	10^{-6}	0.795	1.44	49.8	100
		10^{-5}	0.849	1.35	46.7	100
		1.9×10^{-4}	0.879	1.31	45.5	100
		10^{-3}	0.914	1.26	43.6	100
		10^{-2}	0.954	1.20	41.5	99.5
		10^{-1}	1.02	1.13	39.1	99.8
20	280–300	10^{-6}	0.657	3.14	58.2	100
		10^{-5}	0.690	2.99	55.4	100
		1.9×10^{-4}	0.732	2.82	52.2	100
		10^{-3}	0.756	2.73	50.6	100
		10^{-2}	0.825	2.49	46.1	99.6
		10^{-1}	0.930	2.20	40.7	99.2

Table 7: Hardness parameter calculations for neutron spectra in CMS

r[cm]	E_{min}[MeV]	κ	fluence[10^{-3} cm^{-2}/event]	[%]	damage [%]
11.5	10^{-10}	0.249	5.57	100	100
16.5		0.192	5.86	100	100
30		0.191	5.55	100	100
40		0.171	5.49	100	100
50		0.164	5.21	100	100
60		0.177	5.19	100	100
70		0.160	5.03	100	100
strip	average:	0.173		100	
30	10^{-6}	0.379	2.80	50.5	100
	10^{-5}	0.435	2.44	44.0	100
	1.9×10^{-4}	0.542	1.95	35.1	99.7
	10^{-3}	0.582	1.82	32.8	99.9
	10^{-2}	0.713	1.48	26.7	99.6
	10^{-1}	0.924	1.13	20.4	98.5
60	10^{-6}	0.381	2.41	46.4	100
	10^{-5}	0.431	2.13	41.0	100
	1.9×10^{-4}	0.524	1.76	33.9	100
	10^{-3}	0.585	1.57	30.3	100
	10^{-2}	0.717	1.28	24.7	99.9
	10^{-1}	0.912	0.992	19.1	98.5
70	10^{-6}	0.346	2.33	46.3	100
	10^{-5}	0.396	2.03	40.4	100
	1.9×10^{-4}	0.494	1.63	32.4	100
	10^{-3}	0.563	1.43	28.4	100
	10^{-2}	0.692	1.16	23.1	99.7
	10^{-1}	0.893	0.886	17.6	98.3

Table 8: Hardness parameter calculations for neutron spectra in ATLAS SCT. The differential fluences have been integrated over z. Radial distances correspond approximately to the pixel layer and barrel regions in the Cosener's House layout.

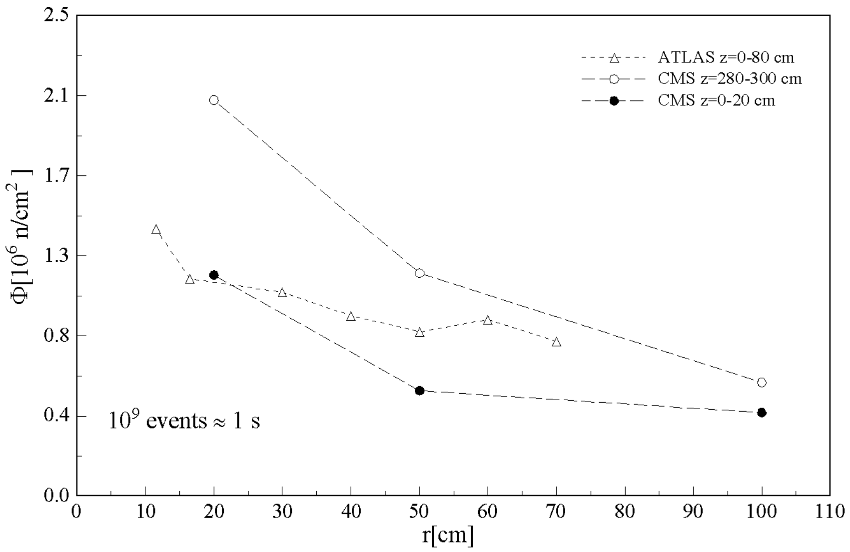

Figure 11: 1 MeV equivalent neutron fluences in CMS and ATLAS corresponding to different distances on the radius. Normalization has been considered to 10^9 events, i.e. approximately one second.

4 The NIEL hypothesis and other particles

Radiation hardness studies for other particles except neutrons have been less systematic. They used proton beams with energies from a few tens of MeV (Hamburg), hundreds of MeV (at LAMPF, TRIUMF, Saclay) to tens of GeV (CERN), and pion beams in the momentum range 100–400 MeV/c.

As we have seen in section 1.2, radiation effects in silicon due to protons and pions are less well characterised. The NIEL damage function [22] for protons is based on calculations and experiments before 1988 [19, 20, 21], and for pions the function is purely theoretical and approximate. Later tentatives [35, 36] try to introduce the effect of the πN resonance into the NIEL dependence, but better results are expected only after detailed simulations (new codes are in preparation [41]) will be performed and compared to experimental results.

The validity of the NIEL hypothesis using van Ginneken's NIEL function is confirmed experimentally with good approximation for protons [22], while for pions new calculations are expected to give a more reliable description. According to [22], the pion damage function is approximately constant, which is surely not true in the energy region of the πN resonance and clearly underestimates the damage for this energy range. In the pion experiments up to now, no correlation based on NIEL is preferred, or values from [35] have been used for κ.

Conclusions

The NIEL hypothesis offers a possible way of correlation and unification of the experimental data in radiation hardness studies on silicon detectors. The scaling with the non-ionising energy loss allows the discussion of the global bulk effects, independent of particle type and the spectrum of the incident beam.

1. The most important element in the discussion on the calculations of the scaling factor (the hardness parameter κ) is the damage function D(E) or NIEL. These functions are tabulated in literature for neutrons, protons, pions, muons, electrons and photons. The case of neutrons is the best known, based on extensive experimental data, at least for the energy range below 20 MeV.

2. New calculations of the hardness parameter have been performed for the spectra of the neutron sources used in radiation hardness tests, as well as for the fields expected at CMS and ATLAS, on the spectra simulated by Monte–Carlo codes for the design of the respective experiments. The variation of κ with different energy cuts (integration limits) has been determined. A summary on the main characteristics of the irradiation facilities, including the hardness factor is given in table 9.

Source	<E> [MeV]	$d\Phi/dt$[n/cm^{2}s^{-1}]	κ^a	κ^b
$\Sigma\Sigma$	0.82	3.385×10^9	0.663	0.66–0.70
PSAIF	0.062	1.23×10^{10}	0.025	$\sim$ 1–1.08
elastic thresh.	1.32	5.81×10^8	0.502	
140 keV	1.99	3.19×10^8	$(0.78\pm0.04)^c$	
ISIS^d	6.44–14.20	5.0×10^7–3.6×10^8	1.00 ± 0.05	1.02–1.5
Lowell	1.06	1.1×10^9	0.90	
T(p,n)^{3}He	1.2	10^7	0.86 ± 0.03	0.88
IBR–2	1.60	3×10^8	0.9–1.05	1.05
Be(d,n)B	5.2	5×10^8	1.46 ± 0.03	1.53
D(d,n)^{3}He	5	1.5×10^7	1.68 ± 0.03	1.60
T(d,n)^{4}He	14.1	6×10^8	1.93 ± 0.06	1.88

Table 9: Main characteristics of neutron irradiation facilities used or damage studies of silicon detectors. (^{a})= κ this work; (^{b})=κ in literature; (^{c})= $\kappa^\dagger$; (^{d})= average value or limit values for the three geometries, on spectra with spline interpolation and high cut at 720 MeV)

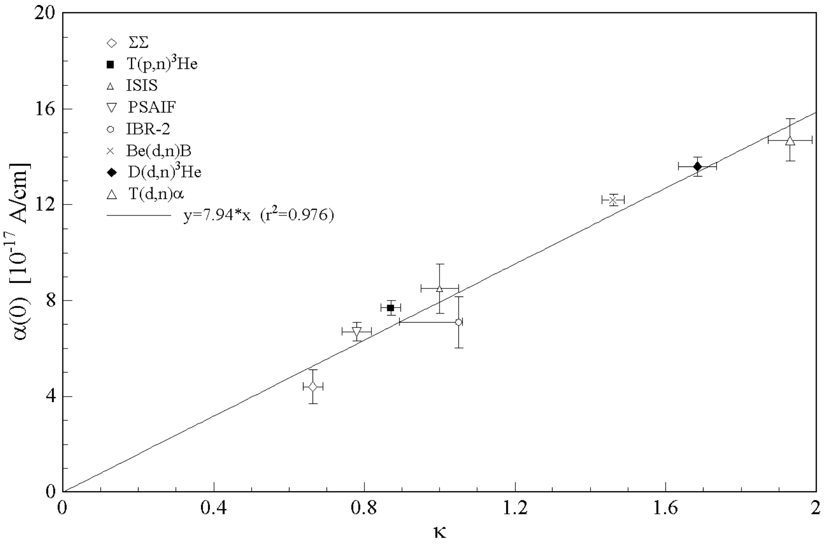

Figure 12: Revised systematic on the current related damage constant $\alpha(0)$ with new hardness parameter κ values

3. The experimental data on damage constants can be correlated in the NIEL scaling.

   - An example for neutrons is given in fig. 12, based on the new κ values from table 9. The revised systematic on $\alpha(0)$ shows a much better agreement. A straight line fit is possible, which gives for $\alpha(0)$ the dependence

   $$\alpha(0) = 7.94 \times \kappa \qquad (r^2 = 0.976)$$

   - The proton damage results support also the NIEL hypothesis [1].
   - For pions and high energy neutrons there are a few questionmarks related to the correctness of the NIEL damage function, especially for pions in the region of the πN resonance. New codes for simulation of the pion damage are in preparation, which will hopefully solve the problem of the scaling for the whole energy range.

References

[1] Angela Vasilescu – Detectors for the study of the proton–proton interaction at very high energies, PhD Thesis, Bucharest (1997) (in Romanian), a summary in English is available as ROSE/TN/97–1

[2] Angela Vasilescu – Overview on the radiation environment in ATLAS and CMS SCT and the irradiation facilities used for damage tests, ROSE/TN/97–3

[3] ASTM E722-85: Standard practice for characterizing neutron fluence spectra in terms of an equivalent monoenergetic neutron fluence for radiation hardness testing of electronics
ASTM E772-93 (revision 1993)

[4] Tatiana Angelescu,..., Angela Vasilescu,... – Radiation hardness studies on silicon detectors in fast neutron fields, Nucl. Instrum. and Meth. A 357 (1995) 55

[5] Tatiana Angelescu, Angela Vasilescu – Comparative radiation hardness results obtained from various neutron sources and the NIEL problem, Nucl. Instrum. and Meth. A 374 (1996) 85

[6] E. Fretwurst et al. – Nucl. Instrum. and Meth. A 342 (1994) 119

[7] Renate Wunstorf – Systematische Untersuchungen zur Strahlenresistenz von Silizium Detektoren für die Verwendung in Hochenergiephysik Experimenten, Int. Rep. DESY FH1K-92-01 (1992)

[8] A. Chilingarov et al. – Nucl. Instrum. and Meth. A 360 (1995) 432

[9] K. Gill et al. – Nucl. Instrum. and Meth. A 322 (1992) 177

[10] S.J. Bates – The effects of proton and neutron irradiations on silicon detectors for the LHC, Dissertation, University of Cambridge, UK, RALT-006 (1993)

[11] Sakuntala Sotthibandhu – Radiation damage studies of silicon detectors, Thesis, Imperial College London, UK, RALT-025 (1994)

[12] M.T. Robinson, I.M. Torrens – Phys. Rev. B 9 (1974) 5008

[13] G.P. Mueller, C.S. Guenzer – IEEE Trans. Nucl. Sci. NS-27, no.6 (1980) 1474

[14] J. Lindhard et al. – Danske Vidensk. Selsk. Mat.-Fys. Medd. 33 (1963) 10

[15] C.A. Coulter, D.M. Parkin – Journal Nucl. Mat. 88 (1980) 249
D.M. Parkin, C.A. Coulter – Trans. Am. Nucl. Soc. 27 (1977) 300
D.M. Parkin, C.A. Coulter – Journal Nucl. Mat. 85&86 (1979) 611

[16] E.E. Conrad – IEEE Trans. Nucl. Sci. NS-18, no.6 (1971) 200

[17] V.C. Rogers et al. – IEEE Trans. Nucl. Sci. NS-22, no.6 (1975) 2326, NS-23, no.1 (1976) 875

[18] A.I. Namenson et al. – IEEE Trans. Nucl. Sci. NS-29, no.1 (1982) 1018

[19] E.A. Burke et al. – IEEE Trans. Nucl. Sci. NS-33, no.6 (1986) 1276

[20] G.P. Summers et al. – IEEE Trans. Nucl. Sci. NS-34, no.6 (1987) 1134

[21] C.J. Dale et al. – IEEE Trans. Nucl. Sci. NS-35, no.6 (1988) 1208

[22] A. van Ginneken – Non ionizing energy deposition in silicon for radiation damage studies, Fermi Nat. Accelerator Lab. report FN-522 (1989)

[23] M.S. Lazo et al. – Sandia Nat. Lab. Tech. rep. SAND 87-0098, vol.1, Proc. Fast Burst React. Workshop 1986, p.85

[24] A.M. Ougouag et al. – IEEE Trans. Nucl. Sci. NS-37, no.6 (1990) 2219

[25] R.E. Mac Farlane – NJOY – A code system for producing pointwise and multigroup neutron and photon cross sections from ENDF/B-IV and -V evaluated nuclear data, RSIC PSR-118, Los Alamos Nat. Lab. (1979)
R.E. Mac Farlane, D.W. Muir – The NJOY nuclear data processing system, version 91 (1994), Los Alamos Nat. Lab. report LA–12740–M

[26] R. Kinsey (ed.) – Evaluated Nuclear Data Files ENDF/B-V, Brookhaven Nat. Lab. (1979), BNL–NCS–50496

[27] M. Tavlet, M.E. Leon-Florian – PSAIF: The PS–ACOL irradiation facility at CERN, RADECS 91, First European Conference on Radiation and its Effects on Devices and Systems, La Grande-Motte, France

[28] M.S. Lazo, SAIC Albuquerque, A. Ougouag, Idaho Falls Nat. Lab., R. Mac Farlane, Los Alamos Nat. Lab. – private communications 1995

[29] R.K. Frank, J.B. Robertson – Solid State Comm. vol.5 (1967) 479

[30] G. Lindström – seminar presented at Bucharest University and INPE, June 1996

[31] P.A. Aarnio et al. – FLUKA 86 User's guide, CERN TIS-RP 168 (1986), and updates (1992)

[32] A. Ferrari et al. – Can we predict radiation levels in calorimeters? – EAGLE int. note CAL-NO-005 (1991), 2^{nd} Int. Conf. on Calorimetry in HEP, Capri (1991)
A. Ferrari et al. – Radiation Calculations for the ATLAS Detector and Experimental Hall – CERN-EST/96-01 (LEA), to be published in Proceedings of the Workshop on Simulating Accelerator Radiation Environment, CERN, Oct. 9–12, 1995

[33] A. Ferrari, CERN, private communications

[34] G.W. Gorfine, G. Taylor – Particle fluxes and damage to silicon on the ATLAS inner detector, int. note INDET-NO-030 (1993)
G.W. Gorfine – Studies of radiation levels in the Large Hadron Collider and of radiation damage to silicon detectors, University of Melbourne, Australia, Thesis (1994)

[35] M. Huhtinen, P.A. Aarnio – Nucl. Instrum. and Meth. A 335 (1993) 580

[36] I. Lazanu et al. – Nucl. Instrum. and Meth. A 388 (1997) 370

[37] P.A. Aarnio, M. Huhtinen – Nucl. Instrum. and Meth. A 336 (1993) 98

[38] M. Huhtinen, CERN, private communications

[39] The CMS Collaboration – CMS: The Compact Muon Solenoid, CERN/LHCC 94–38, LHCC/P1 (1994), Technical proposal

[40] The ATLAS Collaboration – ATLAS SCT – INDET-NO-085 int. rep. (1995)
ATLAS: Technical proposal for a general–purpose *pp* experiment at the Large Hadron Collider at CERN, CERN/LHCC 94–43, LHCC/P2 (1994)

[41] P.A. Aarnio et al. – Nucl. Instrum. and Meth. A 360 (1995) 521

[42] G. Lindström, private communications